

BNL--44548

DE91 011723

**Instabilities of Bellows: Dependence on  
Internal Pressure, End Supports, and Interactions  
in Accelerator Magnet Systems\***

R.P. Shutt and M.L. Rehak  
Brookhaven National Laboratory  
Accelerator Development Department  
Upton, New York 11973

**Abstract**

For superconducting magnets, one needs many bellows for connection of various helium cooling transfer lines in addition to beam tube bellows. There could be approximately 10,000 magnet interconnection bellows in the SSC exposed to an internal pressure. When axially compressed or internally pressurized, bellows can become unstable, leading to gross distortion or complete failure. If several bellows are contained in an assembly, failure modes might interact.

If designed properly, large bellows can be very feasible possibility for connecting the large tubular shells that support the magnet iron yokes and superconducting coils and contain supercritical helium for magnet cooling. We present here (1) a spring-supported bellows model, in order to develop necessary design features for bellows and end supports so that instabilities will not occur in the bellows pressure operating region, including some margin, (2) a model of three superconducting accelerator magnets connected by two large bellows, in order to ascertain that support requirements are satisfied and in order to study interaction effects between the two bellows. Reliability of bellows for our application will be stressed.

**Summary and Conclusions**

In this paper we are dealing with internally pressurized bellows which are to be used extensively for SSC magnet interconnections. In Section II we show how an internally pressurized bellows whose ends are not free to move but are

supported more or less rigidly can become unstable at some well-determined critical pressure  $p_{cr}$ , similarly to a bar that is compressed axially, resulting in Euler-type buckling.

Interconnection bellows must not only accommodate helium coolant flow and pressures, but also must be axially precompressed when warm and extended when cold in order to allow for the thermal shrinkage of superconducting magnets during cooldown. From manufacturers one can obtain pressure ratings, spring constants, diameters, length, convolution geometry, cycling fatigue properties and manufacturing inaccuracies. Large numbers of small or large, and expensive, bellows will be needed, and they must not fail since need for replacement will mean a major interruption of accelerator operation.

In Section III bellows ends are assumed to be supported by two kinds of springs, namely springs acting perpendicularly to the bellows axis and others acting torsionally, providing a torque when the bellows ends' angle is varied. If the torsion springs were not provided, the ends would be considered "hinged". This "spring-support" model has provided much insight into the various conditions under which a bellows can become unstable. The importance of proper bellows support becomes apparent, in addition to selection of proper bellows design parameters. Manufacturing inaccuracies resulting in prebent shapes of purchased bellows, and installation inaccuracies resulting in lateral or angular offsets of bellows ends are also investigated. Instabilities are due to the mentioned Euler-type buckling and end support spring properties. End-to-end offsets and initial bellows prebends (before installation) reinforce these instabilities and

Work performed under the auspices of the U.S. Department of Energy

MASTER

increase bellows distortions and stresses even at operating pressures.

In Section IV, we have studied a model consisting of three magnets interconnected by two bellows. Each magnet can be supported by up to five supports whose lateral stiffness is taken into account in addition to the magnet stiffness. (Vertical magnet support stiffness is larger than lateral.) A resulting magnet end stiffness can then be calculated and used for comparison with the spring-support model discussed in Section III. In particular, however, interactions between bellows are of interest here; what is the effect of a buckling bellows on bellows in neighboring interconnections? To answer this question, we have also introduced the possibility of large forces acting at bellows ends in a direction perpendicular to the magnet axis. This would model the effect of a grossly distorted, but still pressurized, bellows on the magnet system. Since the effect is transmitted through supported magnets, the number and stiffness of magnet supports will thus also play an important role.

Calculations were performed using a symbolic algebra manipulation code called MACSYMA which has been extremely valuable in solving the many algebraic equations following from the previous Sections. The program provided matrix inversions and thus algebraic solutions or matrix coefficients which could be entered into a numerical FORTRAN program. The algebraic solutions for the spring-support model allowed us to understand many of the features that can cause bellows collapse or rupture.

In Section V we discuss numerical results as well as some algebraic expressions including limiting values for some quantities such as spring values.

In the spring-support model we find that a prebent shape of a bellows (we use sine, cosine and parabolic shapes) can stimulate the instabilities that may algebraically appear as indeterminate, even for ideally straight shapes. Our bellows are "designed" for the first instability to occur at a lowest pressure of 450 psi. (Another "peak" will then appear at 1800 psi, and more at still higher pressures.) We are mostly concerned that the stresses or strains in the bellows walls will not exceed specifications. An indication is the maximum axial compression or elongation, uniform for a whole bellows or localized somewhere along the bellows convolution. We therefore present maximum convolution elongations found in the calculations, which are compared with manufacturers' specifications. As the pressure is raised in a bellows wall, elongations increase gradually and can reach large values at our critical pressure of 450 psi. To us the value reached at our maximum operating pressure of 300 psi is particularly important. Thus, after a bellows is designed for the critical pressure, we must also meet the criterion not to exceed allowable elongation at operating pressure, which is determined by the rate of rise of the elongation vs. pressure function.

The rise rate is very much affected by the end support of a bellows. The two ends may be forced into laterally or angularly

offset positions during installation. Furthermore, equivalent lateral and torsional spring properties of the support structure play a very important role. These spring properties produce additional peaks, usually at higher pressure, but also below 450 psi if, especially, the torsional support is not stiff enough. Torsional stiffness as high as  $5 \times 10^5$  lb inch/radian is required for some of the large bellows and magnets considered here, independent of lateral stiffness or pressure. Fortunately, we can easily provide values  $> 10^7$ .

Due to the possible end offsets and due to "support peaks" the rise rate of the bellows elongation increases: support peaks can be placed above 450 psi by sufficient torsional stiffness of end supports. However, the presence of the support peaks increases the rise rate of elongation vs. pressure. The presence of pre-bent shapes additionally increases the rise rate.

The spring support model findings recur in the magnet assembly model (Section IV).

The magnet assembly model allows us to study the effects of one bellows on a neighboring one. Any such effects would, of course, also depend on the rigidity of the magnet supports. Using Fermilab supports, we find that interactions are very small in the pressure region ( $\leq 450$  psi) of interest to us.

One can simulate a "catastrophe" at one bellows by applying one or more large forces there laterally and look at the distortion of the neighboring one. We show that such a disturbance in one bellows affects the other one little at or below operating pressure.

Our general conclusion is that, with sufficient attention to bellows design and support detail (also including the magnet supports if large bellows are used), practically all sizes, large or small, of bellows can be used for interconnections between magnets. However, we recommend strongly that any of the bellows that are to be used in the large quantities required for the accelerators should still be tested very carefully in test set-ups that simulate conditions to which the bellows will be exposed.

## I. Introduction

Bellows represent one of the most commonly used components in engineering structures. They are used to contain vacuum, or gases or liquids under pressure. They can provide for accommodation of differences in thermal expansion between different structures. Bellows can be bent, stretched, or compressed in various ways when used to connect adjoining but not well-aligned assemblies. They can be obtained in a multitude of shapes, sizes, and materials. They may consist of single or multiple layers.

Many applications of bellows merely require design of adjoining components, resulting specifications for connecting bellows, and making proper selections from catalogues available

from a large number of manufacturers. In other cases, special, not readily available bellows may have to be manufactured.

As vital components in much of modern technology, bellows must be as carefully considered in design as other parts in an assembly. They must satisfy all requirements, including a sufficient margin. They must not be overstressed in any direction, must not be damaged in transit, during installation or operation. They must not leak gases or fluids, and their ends must be properly supported. Material fatigue must be taken into account if cycling is intended.

When axially compressed or internally pressurized, bellows can become unstable, leading to gross distortion or complete failure. If several bellows are contained in an assembly, failure modes might interact. (Of course, external pressure can also "buckle" a bellows, but only similarly to a plain cylinder.)

In particle accelerators used for high energy physics research, bellows have been used successfully for a long time to connect beam tubes passing through magnets whose magnetic field, interacting with accelerated electrically charged particles, provides the required circular paths for the particles. In recent times, accelerator magnets have been built to be superconducting (Tevatron at Fermilab, HERA at DESY). In the design stage in the U.S.A. are the Superconducting Super Collider (SSC) in Texas and the Relativistic Heavy Ion Collider (RHIC) at Brookhaven National Laboratory. RHIC will contain many hundreds of superconducting magnets and SSC about 10,000.

For superconducting magnets, one needs many bellows for connection of various helium cooling transfer lines in addition to beam tube connecting bellows.

Large bellows are also considered as a very feasible and strong possibility for connecting the large tubular shells that support the magnet iron yokes and superconducting coils and contain supercritical helium for magnet cooling. In principle, every magnet could be self-contained, with endplates closing off the ends of the shells. These endplates would then be connected by much smaller bellows for the beam tube connections and other bellows to pass cooling fluid, electric bus bars, and instrumentation connections. However, the space available in the magnet interconnection region may be quite limited, and to reduce it further by introduction of the mentioned end plates, transitions, extra bellows, etc., would seem not justified unless it turns out that direct magnet connection with large bellows is not feasible.

It should be mentioned that, with large interconnection bellows full use is made of available volume to limit helium pressure increase when a magnet "quenches", when much of the magnetic field energy is transferred to the helium coolant in a short time. In this event a helium reservoir, such as the interconnection volume, also serves to reduce pressure by reduction of temperature due to partial mixing and helium compressibility.

Assuming that a large bellows has been designed properly concerning stresses, support, availability, etc., we intend to present in this report, (1) a spring-supported bellows model, in order to develop necessary design features for bellows and end supports so that instabilities will not occur in the bellows pressure operating region, including some margin, (2) a model consisting of three superconducting accelerator magnets connected by two large bellows, in order to ascertain that support requirements are satisfied, and in order to study interaction effects between the two bellows. Reliability of bellows for our application will be stressed.

## II. Basic Derivation for Bellows under Pressure

Here we wish to derive an analytic expression which will take into account the possibly destabilizing effect of internal pressure on a bellows. (External pressure has a stabilizing effect up to a limit.) The bellows will be assumed to have an arbitrarily bent shape before installation, due to manufacturing inaccuracies. For simplicity, the bent bellows axis is to remain in a plane.

The ends of the bellows are to be quite rigidly supported but are to be open towards adjoining pipes. Figure 1 shows an element of a bellows with average diameter  $D$ , local axial bend-radius  $\rho$ , and length  $\Delta s = \rho \Delta \chi$ . Pressure  $p$  produces a force  $df_o = p dA$  on element  $dA$  of the bellows wall, when integrated over convolutions, as for a plain cylinder. (Local forces due to pressure inside convolutions will be treated below.) With  $dA = \frac{1}{2}(D d\psi \Delta s_w)$ , where  $\Delta s_w =$  length along wall at angle  $\psi$ , and expressing

$$\Delta s_w = \left( \rho + \frac{D \cos \psi}{2} \right) \Delta x ,$$

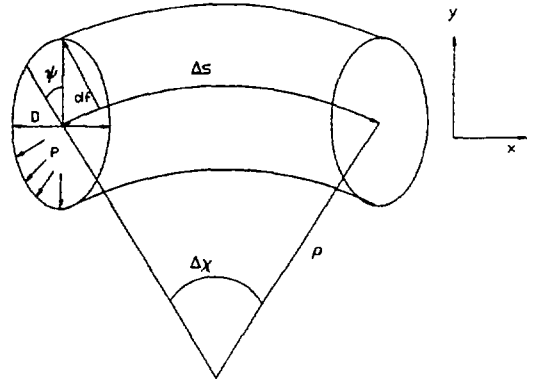


Figure 1.

we obtain for the component of  $df_o$ , in a direction that is parallel to the bending plane,

$$df = p \frac{D}{2} \cos \psi \left[ \rho + \frac{D \cos \psi}{2} \right] d\psi \Delta x.$$

Integration from  $\psi = 0$  to  $2\pi$  results in

$$\Delta f = \frac{\pi D^2 p}{4} \Delta x$$

for the total force due to  $p$  on the length element  $\Delta s$ . (Integral of components of  $df_0$  perpendicular to the bending plane is zero.) Note that this force depends only on the bending angle  $\Delta x = \Delta s/\rho$ . Using Cartesian coordinates,

$$\begin{aligned} \frac{1}{\rho} &= \frac{y''}{(1 + y'^2)^{3/2}} \\ \Delta s &= (1 + y'^2)^{1/2} \Delta x \\ \Delta f &= \frac{\pi D^2 p}{4} \frac{y'' \Delta x}{(1 + y'^2)} \end{aligned}$$

We will be interested only in small bellows deflections. Large deflections are not admissible because wall bending stresses become large and, also the bellows may then interfere with various structures contained in it. Therefore simply

$$\Delta f = -\frac{\pi D^2 p}{4} y'' \Delta x \quad (1)$$

( $x, y$  plane to coincide with bending plane) which now acts only in the  $y$ -direction, neglecting small components along  $x$ . The negative sign is used here since we shall assume that  $df > 0$  when  $y''$  is  $< 0$ .

We can now set up the equation for bending of a bellows under pressure. In Fig. 2, the central axis of a bellows is shown in an arbitrarily bent plane shape supported by forces  $\pm F_{x0}$ ,  $\pm F_{y0}$  and moments  $M_{c1}$  and  $M_{c2}$ , where

$$-M_{c1} + M_{c2} - F_{x0}y(0) + F_{y0}\ell - \int_0^\ell (\ell - x') df = 0 \quad (2)$$

for equilibrium. Here, the bellows is assumed to be straight, not preshaped before installation.

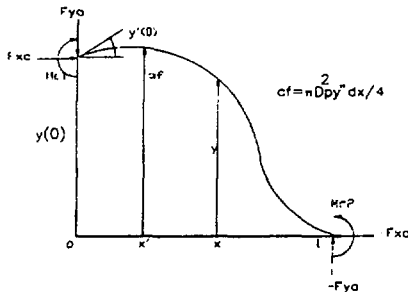


Figure 2.

Bending deflection  $y$  at  $x$  can be found by solving the differential equation

$$y'' = -\frac{M}{EI} = \frac{1}{EI} \left[ F_{x0}(y(0)-y) - F_{y0}x + M_{c1} + \int_0^x (x-x') df \right] \quad (2)$$

where  $E, I$  are "equivalent" values for a bellows represented by a cylinder as discussed below. According to eq. 1

$$\begin{aligned} \int_0^x (x-x') df &= -\frac{\pi D^2 p}{4} \int_0^x (x-x') y''(x') dx' \\ &= -\frac{\pi D^2 p}{4} (y''(x')(x-x') + y'(x')) \Big|_0^x \\ &= -\frac{\pi D^2 p}{4} (y(x)-y(0)-y'(0)x) \end{aligned}$$

Therefore

$$y'' = \frac{1}{EI} (F_{x0}(y(0)-y) - F_{y0}x + M_{c1}) \quad (4)$$

where

$$F_x = F_{x0} + \frac{\pi D^2 p}{4} \quad (4a)$$

$$F_y = \left[ F_{y0} - \frac{\pi D^2 p}{4} y'(0) \right] \quad (4b)$$

$F_{x0}$  is the axial bellows end support force before pressure is introduced, for instance due to axial precompression.  $F_{y0}$  gives lateral support at  $x = 0$ .  $y(0)$  and  $y'(0)$  are given as boundary conditions or can be determined as a part of the solution of eq. 4. Assume, for instance, that we give as boundary conditions at  $x = 0$

$$\begin{aligned} y &= y(0) \\ y' &= y'(0) \end{aligned}$$

and at  $x = \ell$

$$\begin{aligned} y &= y(\ell) \\ y' &= y'(\ell) \end{aligned}$$

Solution of eq. 4 requires determination of two integration constants. Furthermore we must find  $M_{c1}$  and  $F_{y0}$ . Thus the four boundary conditions suffice. Moment  $M_{c2}$  can be found from eq. 2, if required.

Equation 4 is an Euler-type equation describing the effect of an axial end force  $F_x$  on a bar. For a sufficiently large end force buckling can occur. Thus, for a bellows internal pressure  $p$  can result in buckling ("squirming"), if the bellows is supported at the ends as was assumed.

So far we have neglected the effect of shear forces on bending of the bellows. Axially, the bellows acts like a spring

whose spring constant depends on various parameters. To be called "K", it will be derived below. Laterally, without bending, the bellows must act approximately like a cylinder of diameter D with the bellows convolution wall thickness t, but with a much smaller equivalent elastic modulus than that of a cylinder.

$$EI = \frac{KD^2\ell}{8} \quad (6c)$$

It follows that

$$P_{cr} = \left[ \left( 1 + \frac{2\pi KD}{0.4\ell E_s} \right)^{1/2} - 1 \right] \frac{0.4\pi Dt E_s}{2}$$

Considering bending of a bar whose ends are fixed and which is loaded axially by forces  $\pm F$ , a critical force  $F_{cr}$  exists where the bar becomes unstable. A simple expression, due to Euler gives eq. 5,

$$F_{cr} = \frac{4\pi^2 E I_r}{\ell_r^2} \quad (5)$$

where  $E_r$ ,  $I_r$ ,  $\ell_r$  are elastic modulus, moment of inertia of cross section, and length, respectively. Ends are assumed to be fixed. Equation 5 does not take shear forces into account. An expression taking deflections due to both bending and shear forces into account has been given by Timoshenko<sup>[1]</sup>. The critical force is now expressed by

$$P_{cr} = \left[ \left( 1 + \frac{16\pi^2}{\ell_r^2} \frac{E I_r}{A_r G_r} \right)^{1/2} - 1 \right] \frac{A_r G_r}{2} \quad (6)$$

where  $A_r$  and  $G_r$  are cross section and shear modulus of the bar.

Concerning pure shear, we have to treat the bellows as a cylinder whose average cross section is  $A_r = \pi Dt$ .

$$G_r = \frac{E_s}{2(1+\nu)}$$

where  $E_s$  will be the elastic modulus of the bellows material. If  $\nu = 0.25 =$  Poisson's ratio,  $G_r = 0.4 E_s$ .

The product  $E_r I_r$  concerns the axial behavior of the bellows. Particularly,  $E_r$  must be an "equivalent" number referring to the axial bellows spring constant K. The spring constant (also called "stiffness") of a bar would be

$$K = \frac{\text{Elastic modulus} \times \text{cross section}}{\text{length}}$$

For a spring, or bellows, one can define then an equivalent elastic modulus

$$E = \frac{K\ell}{A} \quad (6a)$$

if K is given. ( $A = A_r$ ,  $\ell = \ell_r$ ). Therefore, in eq. 6 we will set  $E_r = E$ .  $I_r$  will have an average value

$$I_r = I = \frac{\pi}{64} \left[ \left( D + \frac{t}{2} \right)^4 - \left( D - \frac{t}{2} \right)^4 \right] = \frac{\pi D^3 t}{8} \quad (6b)$$

if  $t \ll D$ . Therefore

Typical average values for bellows considered in this report will be

K	= 3000 lbs./inch
D	= 13.5" or less
$\ell$	= 10" or less
t	= 0.03"
$E_s$	= $3 \times 10^7$ psi

which results in

$$\frac{16\pi^2}{\ell^2} \frac{EI}{AG_r} = \frac{2\pi KD}{0.4\ell E_s} = 0.071 \ll 1$$

Therefore it follows from eq. 6 that

$$P_{cr} \approx \frac{4\pi^2 EI}{\ell^2} = P_{cr} \quad (6d)$$

for our case; deflections due to shear are small here, thus justifying the simple approach taken to derive eq. 3. The reason is that here  $E_r \ll G_r$ . If D were considerably larger or  $\ell$  smaller, eq. 6 would have to be used. Equation 5 gave the critical buckling force  $F_{cr}$  at the ends of a bar which are fixed.

For our calculations we will not be allowed to assume that ends are rigidly fixed; the bellows will be welded to magnet ends which are somewhat flexible, laterally as well as rotationally. Therefore we will encounter buckling modes where

$$F_{cr} = \frac{\pi^2 EI}{\ell^2}$$

Making use of eq. 6c,

$$F_{cr} = \frac{\pi^2 KD^2}{8\ell} \quad (7)$$

Thus, in order not to exceed the critical state we must demand that

$$K \geq \frac{8\ell F_{cr}}{\pi^2 D^2} \quad (8)$$

At installation, at room temperature, bellows will be precompressed by an amount  $\lambda$ . Magnets and bellows are designed for a maximum operating pressure  $p_{op}$ . Adding some margin to  $p_{op}$  we obtain  $p_{cr}$ . Then we can set

$$F_{cr} = K\lambda + \frac{p_{cr}\pi D^2}{4} \quad (9)$$

from which follows, with eq. 8,

$$F_{cr} = \frac{\pi D^2 p_{cr}}{4 \left[ 1 - \frac{8\lambda \ell}{\pi^2 D^2} \right]} \quad (10)$$

We can now choose critical pressure  $p_{cr}$  for a bellows and use the resulting  $F_{cr}$  to determine the bellows parameters.

For axial spring constant  $K$  we use eq. 8(10):

$$K = \frac{8\ell F_{cr}}{\pi^2 D^2} \left[ \frac{2\ell p_{cr}}{\pi \left[ 1 - \frac{8\lambda \ell}{\pi^2 D^2} \right]} \right]$$

For a lateral spring constant, both bellows ends fixed to be parallel to bellows axis:

$$K_t = 1.5K \left( \frac{D}{\ell} \right)^2 \quad (11)$$

which can be proved easily by an appropriate bending calculation.

### III. Spring-Supported Bellows Model

In order to understand and explain the behavior of bellows used for interconnecting accelerator magnets, it has been useful to treat a model consisting of a bellows whose ends are supported by springs. These springs are to model the effects on the magnet ends which could be deflected laterally by forces acting perpendicularly to the magnet axis, and rotationally by moments. Both forces and moments can produce lateral deflections as well as rotations of the bellows ends.

For the spring supported bellows model we will use two straight springs at the bellows ends, with spring constants  $k_1$  and  $k_2$  (lbs./inch), and two torsion springs with spring constants  $k_{t1}$  and  $k_{t2}$  (lbs. inch/radian).

Manufactured items can adhere to ideal shapes only within tolerances. Thus, we cannot assume that bellows can be ideally straight but will be obtained pre-bent to some shape that could be expressed by a Fourier series. For our purpose it is not necessary to carry the higher harmonics but it is sufficient to carry two of the lowest ones. The prebent shape shall be

$$y_0 = d_1 \sin \frac{\pi x}{\ell} + d_2 \left[ 1 - \cos \frac{2\pi x}{\ell} \right] \quad (12)$$

with  $d_1, d_2$  the amplitudes,  $\ell$  the bellows length.  $y_0 = 0$  at  $x = 0$  and  $\ell$ . The lowest mode (also representative of a possible offset mode  $d_3 \cos \pi x/\ell$ ) will cause buckling of the bellows at the lowest pressure. The higher mode ( $\cos 2\pi x/\ell$ ) would cause buckling only at 4 times the lowest pressure but it significantly affects the deflections of the bellows, and therefore stresses, even at much lower pressures, in the bellows operating region.

In Section II it was shown that the effect of internal pressure on an arbitrarily shaped bellows can be represented by an axial force that may cause buckling and a lateral force that depends on the pressure and the angle ( $y'(0)$ ) that the bellows axis subtends at  $x = 0$  (see eq. 4a,b).

Figure 3 shows the axis of a bellows, which departs from straightness by a function  $y_0$  such as given in eq. 12. In addition, due to (small) fabrication errors of the bellows mountings, the ends are to be offset laterally by length  $\zeta$ . At the ends, the bellows is mounted on laterally acting springs,  $k_1$  and  $k_2$ , and rotation of the ends is limited by torsion springs  $k_{t1}, k_{t2}$ . The bellows is to be axially compressed by length  $\lambda$  and internally pressurized to pressure  $p$ . The bellows ends are then exposed to equivalent axial end forces (eqs. 4a)

$$\pm F_x = \pm F_a = \pm \left[ \lambda K + \frac{\pi D^2 p}{4} \right] \quad (13)$$

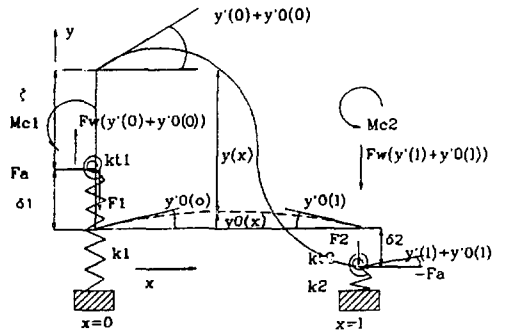


Figure 3.

Lateral support is to be given by forces  $F_1$  and  $F_2$ . Deflection  $y$  is to be measured from the unstressed, prebent shape  $y_0(x)$  of the bellows. If

$$y'(0) + y'_0(0) = 0 \text{ and } y'(\ell) + y'_0(\ell) = 0$$

we have  $F_1 = F_2$ . If the end slopes are not zero, then, similarly to eq. 4b,  $F_1, F_2$  become

$$F_1 = F_1 - F_w \left[ y'_0(0) + y'(0) \right]$$

$$F_2 = F_2 + F_w \left[ y'_0(\ell) + y'(\ell) \right]$$

as the total lateral forces on the bellows ends, due to the spring

supports and non-zero end slopes.  $\left[ F_w = \frac{\pi D^2 p}{4} \right]$  For equilibrium:

$$F_1 + F_2 = F_w \left[ y'(0) - y'(\ell) + \frac{2\pi d_1}{\ell} \right] \quad (14)$$

making use of eq. 12. (Signs in eq. 14 are consistent with Fig. 3.)

Moments  $M_{c1}$ ,  $M_{c2}$  are also required for end support. For equilibrium:

$$M_{c1} + M_{c2} - F_a(\delta_1 - \delta_2) + \left[ F_1 - F_w \left( y'(0) + \frac{\pi d_1}{\ell} \right) \right] \ell = 0 \quad (15)$$

Bending deflections  $y$  at  $x$ , due to the applied forces, are now found from

$$y'' = -\frac{1}{EI} \left[ F_a(y + y_0 - \delta_1) + F_1 - F_w \left( y'(0) + \frac{\pi d_1}{\ell} \right) x + M_{c1} \right] \quad (16)$$

$F_1$  is the force that is due to compression or extension of support spring  $k_1$ . Therefore

$$\delta_1 = \frac{F_1}{k_1}$$

similarly

$$\delta_2 = \frac{F_2}{k_2}$$

For boundary conditions,  $M_{c1}$  and  $M_{c2}$  determine the end slopes due to the bending forces:

$$y'(0) = \frac{M_{c1}}{k_{t1}} \quad (17)$$

$$y'(\ell) = \frac{M_{c2}}{k_{t2}} \quad (18)$$

and for the total end deflections:

$$y(0) = \zeta + \delta_1 = \zeta + \frac{F_1}{k_1} \quad (19)$$

$$y(\ell) = \delta_2 = \frac{F_2}{k_2} \quad (20)$$

Boundary conditions 17 to 20, together with equilibrium conditions 14 and 15 will be used to determine  $y(x)$ . The six conditions suffice to find  $F_1$ ,  $F_2$ ,  $M_{c1}$ ,  $M_{c2}$ , and two integration constants for eq. 16 whose solution is

$$y = A \cos \omega x + B \sin \omega x + C_1 \sin \frac{\pi x}{\ell} + C_2 \cos \frac{2\pi x}{\ell} + Dx + G \quad (21)$$

Substitution into eq. 16 results in

$$\omega = (F_a/EI)^{1/2} \quad (22)$$

and expressions for  $C_1$ ,  $C_2$ ,  $D$ , and  $G$ , while  $A$  and  $B$  are the integration constants that need to be addressed. Of special interest are

$$C_1 = d_1 \left( \frac{\omega \ell}{\pi} \right)^2 / \left[ 1 - \left( \frac{\omega \ell}{\pi} \right)^2 \right] \quad (23)$$

$$C_2 = -d_2 \left( \frac{\omega \ell}{2\pi} \right)^2 / \left[ 1 - \left( \frac{\omega \ell}{2\pi} \right)^2 \right]$$

which are due to the prebent shape of the bellows (see eq. 12). We can therefore expect buckling (squirming) of the bellows when

$$\omega \ell = \pi \text{ if } d_1 \neq 0$$

and

$$\omega \ell = 2\pi \text{ if } d_2 \neq 0$$

or when

$$F_a = \frac{\pi^2 EI}{\ell^2} \quad (24)$$

$$F_a = \frac{4\pi^2 EI}{\ell^2} \quad (25)$$

in agreement with Euler-type buckling.

We must not exceed allowed extension or compression of the bellows, to be called  $\Delta \ell_{\max}$ .

Maximum bellows stress  $\sigma$  due to bending (excluding stress due to local pressure on convolution wall, which must be added).

$$\sigma = -\frac{M}{Z} = \frac{y''EI}{Z} = y'' \frac{K\ell}{2\pi t}$$

Strain  $\epsilon$  is

$$\epsilon = \frac{\sigma}{E} = y'' \frac{D}{2}$$

Thus

$$\Delta \ell = \epsilon \ell = \frac{y'' D \ell}{2}$$

and, including precompression  $\lambda$ :

$$\Delta \ell_{\max} = \lambda + \frac{|y''| D \ell}{2} \quad (26)$$

which must be checked for all cases.

In addition to the buckling modes (eqs. 24, 25) due to bellows prebending, there are important additional ones due to the end supports ( $k_1$ ,  $k_2$ ,  $k_{t1}$ ,  $k_{t2}$ ) which will be considered in detail below, and numerical results are discussed.

#### IV. Bellows Interactions in Magnet Systems.

In Fig. 4 we show schematically three magnets and two bellows interconnecting the magnets. Supports for the magnets are shown at locations  $x_1$  to  $x_{19}$ . Support forces are  $F_1$  to  $F_{19}$ . The whole system is assumed to be preshaped (before applying forces) according to a function  $y_0(x)$ . Deflections  $y_n(x)$  ( $1 \leq n \leq 19$ ) are to be measured, starting at  $y_0(x)$ , so that the total deviation from abscissa  $x$  is  $y_n(x) + y_0(x)$ . Concerning  $y_0(x)$ , dipoles are circularly curved, quadrupoles (packaged together with sextupole and corrector magnets) are straight, but much shorter than dipoles, and interconnections are straight.  $y_0(x)$  shall represent an average curve of the system. For  $1 \leq n \leq 18$ , forces  $F_n$  will be expressed by

$$F_n = k_n \delta_n \quad (27)$$

if the  $k_n$  are the support spring constants, and having called  $\delta_n = y_n(x_n)$ . For  $n = 19$ ,

$$F_{19} = k_{19} y_{18}(x_{19}) \equiv k_{19} \delta_{19} \quad (28)$$

Note that forces  $F_n$  act only approximately in the  $y$ -direction as shown in Fig. 4. For the present problem (small deflections) this approximation is adequate.

Two bellows are located between  $x_6$  and  $x_7$ , and  $x_{13}$  and  $x_{14}$ . At these locations  $k_{6,7,13,14} = 0$  so that there are no magnetic support forces (eq. 27). However, one can apply forces  $F_{6,7,13,14}$  for

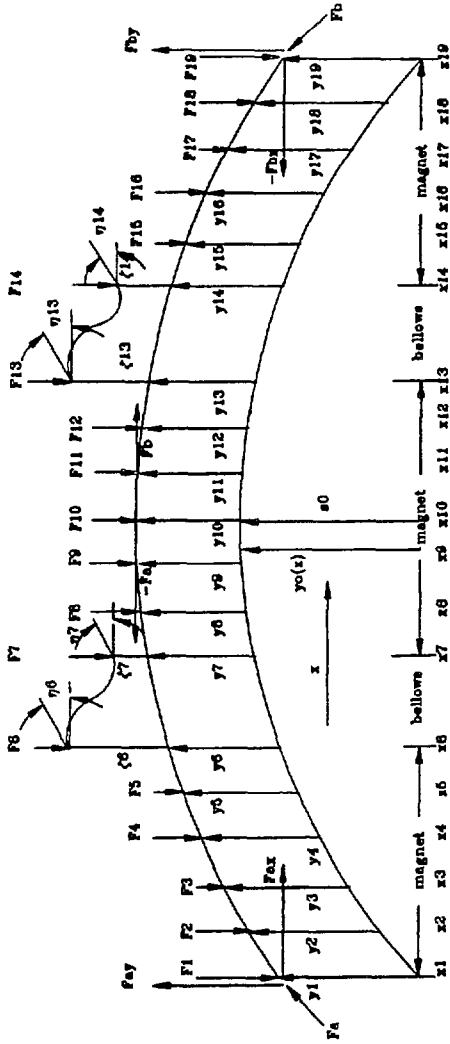


Figure 4.

the purpose of analyzing effects of "bellows catastrophes" on adjacent magnets and other bellows. Such a "catastrophe" may be collapse of a bellows due to buckling, resulting in gross distortion of the bellows and therefore possibly large laterally acting forces due to the internal pressure. When a bellows buckles, it will not necessarily release the pressure in it but rather deform the convolutions until they are either compressed till contact or

"straightened" to become a smooth surface.

In our calculations we assume that large diameter bellows are employed. Therefore forces on bellows and adjacent components can become large. On smaller bellows the forces of concern to us are, of course, also smaller, decreasing proportionally to the average bellows cross section.

In Fig. 4, the bellows ends are shown to be offset laterally from the magnet ends, at  $x_{6,7,13,14}$  by  $\zeta_{6,7,13,14}$  and by angle  $\eta_{6,7,13,14}$ . While adjacent magnets must be aligned within small tolerances, the offsets can be due to inaccuracies of the bellows end mountings or welding procedures.

It has been shown in Section II, eqs. 4a, 4b, that the effects of internal pressure  $p$  on arbitrarily shaped or distorted cylinders or bellows can be calculated by merely applying end forces  $\pm \pi D^2 p / 4$  along the, however deflected, axis of the pressurized container.  $D$ , again, is the inner diameter of a cylinder or average diameter of a bellows. Force components in directions  $x$  and  $y$ , if  $y(x)$  represents the bellows axis, are at  $x = 0$

$$F_x(0) = \frac{\pi D^2 p}{4} (1 - y'(0)^2) = \frac{\pi D^2 p}{4} - F_w$$

if  $y'(0)$  is small, and

$$F_y(0) = \frac{\pi D^2 p}{4} y'(0) - F_w y'(0)$$

Replacing zero by length  $\ell$  gives corresponding expressions at  $x = \ell$ . If additional forces act, we obtain eqs. 4a, 4b. Adding bellows precompression force  $\lambda K$  to  $F_w$  we define

$$F_a = \lambda K + \frac{\pi D^2 p_a}{4} = \lambda K + F_{w_a} \quad (29)$$

which is to act (approximately) in the  $x$ -direction.  $(F_{w_a} y')$  is to act in the  $y$ -direction.  $F_{ax} = F_a$  and  $F_{ay} = F_{w_a} y'_1(x_1)$  are shown at  $x = x_1$ ,  $y = y_1$  in Fig. 4. (Actually bellows precompression force  $\lambda K$  acts at axially fixed location  $x_3$ , but for simplicity we shall locate it at  $x = x_1$ , which is unimportant for this calculation.) In order also to analyze the effect of unequal pressures at magnet ends, as could be encountered during asymmetrical magnet quenches, it is assumed, and shown at  $x = x_{10}$  that force  $-F_a$ , acting at  $x_{10}$ , provides equilibrium (together with the relevant force in the  $y$ -direction) for  $F_a$  at  $x = x_1$ . From here on force

$F_b = \lambda K + \frac{\pi D^2 p_b}{4} = \lambda K + F_{w_b}$  is to act, having replaced pressure  $p_a$

by  $p_b$ . At  $x = x_{19}$ ,  $-F_{bx} = -F_b$  must then act for equilibrium, and  $F_{by} = F_{w_b} y'_{19}(x_{19})$ .

As mentioned above, there are no supports at  $x = x_{6,7,13,14}$  where  $k_{6,7,13,14} = 0$ .  $y_{6,7,13,14}$  indicate deflections at the bellows ends. This leaves magnet supports at the remaining locations. Each of the three magnets is shown with five supports. The actual number of supports for a given magnet can be adjusted

by setting the  $k_n \neq 0$  at the support locations. (Elsewhere  $k_n = 0$ .) Magnet supports can thus be specified by entering known values for the  $k_n$ . We can then analyze SSC dipoles (D) (five supports for magnet to cryostat) and quadrupoles (Q) (three supports). Thus any combination such as DDD, DQD, etc., can be studied. The SSC dipole cryostat is to have only two supports to the floor. This will considerably decrease the system stiffness provided by the five magnet-to-cryostat supports.

We proceed to derive relevant relations for analysis. Refer to Fig. 4. The sagitta  $s_0$  of our system, compared to cord length  $(x_{19} - x_1)$  is found to be very small. Therefore we can approximate the arc by a parabola which is given by

$$y_0(x) = \frac{4s_0}{x_{19}^2} x(x_{19} - x)$$

having called  $x_1 = 0$ .  $4s_0/x_{19}^2$  is the curvature of the system which we shall, for our purpose, merely call approximately equal to the dipole curvature  $\phi = 4s/\ell^2$ , if  $s$  = dipole sagitta,  $\ell$  = length. Therefore

$$y_0(x) = \phi x(x_{19} - x) \quad (36)$$

Referring to Fig. 4, we can now write down differential equations for bending of the magnet and bellows in the 18 regions  $(x_{n+1} - x_n)$ . ( $1 \leq n \leq 18$ .) For simple bending, where length  $>$  height or width of a bar or, as has been shown, for bellows,

$$y_n'' = -\frac{M_n}{E_n I_n}$$

Examples: for region  $(x_2 - x_1)$ :

$$-M_1 = F_0(\delta_1 - y_0(x) - y_1) - F_1(x - x_1) + F_{wa}(y_1'(x_1) + \phi x_{19})x \quad (31)$$

$$\delta_1 = \frac{F_1}{k_1} \quad (32)$$

$$F_{wa} = \pi D^2 p_a / 4$$

$E_1$  = elastic modulus of magnet shell (including Poisson ratio)  $I_1$  = moment of inertia of magnet cross section (combination of shell and yoke laminations).

For region  $(x_7 - x_6)$ : bellows:

$$-M_6 = F_6(\delta_1 - y_0(x) - y_6) - \sum_{v=1}^6 F_v(x - x_v)$$

$$+ F_{wa}(y_1'(x_1) + \phi x_{19})x + \tau_3$$

$$- F_a \left[ d_{cs} \sin \left( \frac{\pi x}{\ell} \right) + d_{cs} \left[ 1 - \cos \left( \frac{2\pi x}{\ell} \right) \right] \right]$$

$\tau_3 = \frac{GI_p}{\ell_p} y_3'(x_3)$  takes into account a torque exerted by the center support of the magnet caused by distortion of the shell resulting in angle  $y_3'$  at  $x_3$ .

$d_{cs}$  and  $d_{cs}$  determine the amount of prebend of the bellows before installation (see Section III, eq. 12). Similarly, for  $d_{13}$ ,  $d_{c13}$  for bellows prebend in region  $x_{14} - x_{13}$ . All other  $d_{nn}$ ,  $d_{cn} = 0$ .

$E_6 = E$  (see eq. 6a)

$I_6 = I$  (see eq. 6b)

A general equation, valid in all regions, can be written:

$$y_n'' = \frac{1}{E_n I_n} \left[ F_n \left\{ \delta_{10} - y_0(x) + y_0(x_{10}) - y_n - d_{cn} \sin \left( \frac{\pi x}{\ell} \right) - d_{cn} \left[ 1 - \cos \left( \frac{2\pi x}{\ell} \right) \right] \right\} - \sum_{v=1}^n F_v(x - x_v) + F_6(\delta_1 - y_0(x_{10}) - \delta_{10}) + v_n + F_{w\phi} \phi x_{19} x \right] \quad (33)$$

In this equation it has been assumed that the slopes  $y_n'(x_n)$  are  $\ll \phi x_{19}$  (slopes at  $x_1 (=0)$  and  $x_{19}$  due to dipole curvature).  $v_n$  shall be the sum of torques that may be exerted by supports, such as  $\tau_3$ :

$$\begin{aligned} \text{for } n=1,2, \quad v_n &= 0 \\ 3 \leq n \leq 9, \quad v_n &= \tau_3 \\ 10 \leq n \leq 16, \quad v_n &= \tau_3 + \tau_{10} \\ 17 \leq n \leq 18, \quad v_n &= \tau_3 + \tau_{10} + \tau_{17} \end{aligned}$$

For  $\tau_{10}$ ,  $\tau_{17}$  replace  $y_3'(x_3)$  by  $y'_{10}(x_{10})$ ,  $y'_{17}(x_{17})$ , respectively. Furthermore,

$$\text{for } 1 \leq n \leq 9: F_n = F_b - F_a \quad F_{w\phi} = F_{wa} = \frac{\pi D^2 p_a}{4}$$

$$10 \leq n \leq 18: F_n = F_b, F_b = F_a$$

Equation 33 represents 18 second order differential equations, requiring determination of 36 integration constants. In addition, values of the support forces  $F_n$  must be determined. These forces are, of course, known to be equal to zero where a support spring constant  $k_n = 0$ , such as at  $x_{6,7,13,14}$  (unless  $F_{6,7,13,14} \neq 0$ ). For the SSC magnets, there are five supports for dipoles and three for quadrupoles. Therefore, at most 15 additional quantities must be found, for a total of 51.

There are two equilibrium conditions for the system; (1)

$\Sigma$  forces = 0, (2)  $\Sigma$  moments = 0.

$\Sigma$  forces:

$$\sum_1^{19} F_v - \frac{\pi D^2}{4} (p_a + p_b) x_{19} \phi = 0 \quad (34)$$

$\Sigma$  moments:

$$F_6(\delta_{10} - y_0(x_{19}) + y_0(x_{10}) - \delta_{10}) - \sum_1^{18} F_v(x_{19} - x_v) + F_a(\delta_1 - y_0(x_{10}) - \delta_{10}) + \tau_3 + \tau_{10} + \tau_{17} + \frac{\pi D^2 p_a}{4} \phi x_{19}^2 = 0 \quad (35)$$

In addition, we need 49 boundary conditions to solve for the mentioned 51 forces and integration constants: as defined,

$$y_n(x_n) = \delta_n = \frac{F_n}{k_n} \quad (1 \leq n \leq 18, n \neq 6,7,13,14) \quad (36)$$

This results in  $18 - 4 = 14$  equations. One additional equation must be

$$y_{18}(x_{19}) = \frac{F_{19}}{k_{19}} \quad (37)$$

Continuity ( $y_n$  to  $y_{n+1}$  "nodes") equations are

$$y_{n+1}(x_{n+1}) - \zeta_{n+1} = y_n(x_{n+1}) \quad (38)$$

$$y'_{n+1}(x_{n+1}) - \eta_{n+1} = y'_n(x_{n+1}) \quad (39)$$

Equations 38, 39 are valid when  $1 \leq n \leq 17$ , therefore result in  $2 \times 17$

= 34 more equations, for a total of 14 + 1 + 34 = 49, as needed. Only  $\zeta_{6,7,13,14}$ ,  $\eta_{6,7,13,14}$  will be  $\neq 0$  for the system drawn in Fig. 4.

Note that, in Fig. 4,  $\zeta_{7,14}, \eta_{7,14}$  are drawn so that they must be entered as negative values; for instance,  $y_7(x_7) - \zeta_7 = y_6(x_7)$ ; since in Fig. 4  $y_7(x_7) < y_6(x_7)$ ,  $\zeta_7$  must be  $< 0$ : for abrupt increases of  $y(x)$  (or  $y'(x)$ ) with  $x, \zeta$  (or  $\eta$ )  $> 0$  and for decreases  $\zeta$  (or  $\eta$ )  $< 0$ .

The solution for equation 33 is

$$y_n(x) = A_n \cos \omega_n x + B_n \sin \omega_n x + C_n x + D_n x^2 \quad (40)$$

$$+ E_{cn} \sin \left[ \frac{\omega_n}{\ell} (x - x_n) \right] + E_{cn} \cos \left[ \frac{2\omega_n}{\ell} (x - x_n) \right] + G_n$$

$$\omega_n = (F_n / E_n I_n)^{1/2}$$

$$C_n = -\frac{1}{F_n} \left[ \sum_{v=1}^n F_v + F_n \phi x_{19} - \phi F_{nd} x_{19} \right]$$

$$D_n = \phi$$

$$E_{cn} = -d_{cn} \left[ \frac{\omega_n \ell}{\pi} \right]^2 \left[ 1 - \left( \frac{\omega_n \ell}{\pi} \right)^2 \right]^{-1}$$

$$E_{cn} = -d_{cn} \left[ \frac{\omega_n \ell}{2\pi} \right]^2 \left[ 1 - \left( \frac{\omega_n \ell}{2\pi} \right)^2 \right]^{-1}$$

$$G_n = \frac{1}{F_n} \left[ F_n - F_\beta \lambda (\delta_{10} + y_\alpha(x_{10})) + F_\beta \delta_1 + \sum_1^n F_v x_v + v_n - 2\phi E_n I_n - F_n d_{cn} \right]$$

The  $A_n, B_n$  are to be determined, together with the  $F_n$ , by solving eqs. 34 to 40.

## V. Numerical results: Spring-Supported bellows model

In order to obtain the bellows deflection ( $y(x)$  (III, eq. 21), one must solve a system of 6 equations formed by the six boundary conditions eqs. 14, 15, 17 to 20 for the 6 unknowns, A, B, Mc1, Mc2, F1, F2. The solution reveals that A and B have a common denominator which is the determinant of the matrix shown in Fig. E1 along with the surface determinant = 0 as a function of pressure and stiffnesses. When the determinant approaches zero,  $y$  becomes unbounded or indeterminate and the bellows is unstable. The determinant is, as expected, a symmetrical expression with respect to left and right since the indices 1 and 2 can be interchanged without altering its value. It is a function of  $F_a$  (both directly and through  $\omega$ , eq. 22) and of  $k_1, k_2, k_{11}, k_{12}$ . With this expression one can find the critical buckling load of the bellows due to the support system only, that is the value of  $F_a$  (or pressure  $p$ ) which will reduce the determinant to zero for given stiffnesses. For simplicity, the realistic assumptions that  $k_{11} = k_{12}$  and  $k_1 = k_2$  are used from now on. The precompression is  $\lambda = 0$ .

Fig. b1 shows a plot of the maximum bellows elongation

defined in eq. 26 as a function of pressure. The bellows was designed to have a critical load at 450 psi due to an assumed initial sine shape (prebend). This determines an axial stiffness of  $K = 2760$  lb/in for a bellows of inner diameter  $D_i = 14.3$  in and length 9.3 in, the supports have assumed stiffnesses of  $k_{11} = 3.7$  lb in/radian and  $k_1 = 7.7$  lb/in. There is a peak at 600 psi and one at 1875 psi. The expected peak, for which the bellows was designed at 450 psi, is absent because  $y$  (eq. 21) is indeterminate (zero appears both in the numerator and denominator). Nevertheless the bellows should be designed as having a critical load at that value since deviations could lead to large deflections. Seidel<sup>(1)</sup> and Haringx<sup>(2,3)</sup> discuss and present experimental data on the stability of internally pressurized bellows. Haringx shows that a bellows with clamped ends can fail at relatively low values for pressure. Keeping in mind that there can be a peak at  $\omega \ell = \pi$ , the spring model will be used here only to find the buckling load due to support details.

We show next how the analysis of the determinant alone allows one to predict the critical load due to the spring supports only. The determinant is solved first for the variable  $k_1$ , the solution is plotted for several values of  $k_{11}$  as a function of  $p$  in Fig. b2. A horizontal line drawn at  $k_1 = 7.7$  lb/in intersects the curve of solutions with  $k_{11} = 3.7$  lb in/radian when  $p$  is about 610 psi. (Curves are truncated at 20000 lb/in.) With  $k_{11} = 0$ ,  $p$  is only somewhat larger, at about 650 psi.

An equivalent way to predict the buckling load is to solve the determinant for the variable  $k_{11}$  as a function of  $k_1$  and  $p$ . There are two solutions since the determinant is a quadratic function of  $k_{11}$ . The first one, denoted  $k_{11a}$  in Fig. b3, shows that a horizontal line drawn at 3.7 lb in/radian would intersect the determinant = 0 curve for  $k_1 = 7.7$  lb/in at 610 psi. The second root, denoted  $k_{11b}$  in Fig. b4 shows that for all values of  $k_1$  the determinant is equal to zero at 1875 psi when  $k_{11} = 3.7$  lb in/radian. We have thus explained the origin of the two peaks in Fig. b1: they can be traced to a given combination of support stiffnesses. Figures b2, b3, b4 can be used to ensure that peaks due to supports remain always above the critical load for which the bellows is designed.

We now give an example where the support peak occurs below the  $\omega \ell = \pi$  peak. Figure b4 predicts that a peak could be obtained at 425 psi if  $k_1 = 7000$  lb/in and  $k_{11} = 1.7$  lb in/radian, this is verified in Fig. b5 which shows the 425 psi peak. In addition there are the peaks at 650 psi and at 1830 psi shown in Fig. b2 and/or b3. Table 1 lists peak locations according to their origin for two values of  $k_{11}$ .

The influence of the mounting offset  $\zeta$  is to accelerate the rate of rise to the peaks, but not to cause them. It is a multiplying factor of the numerator of  $y$  and does not appear in the denominator. The influence of  $\zeta$  can be seen by comparing figs. b6 and b7 which differ only in that  $\zeta = 0.03$  in Fig. b6 and zero in Fig. b7. The first support peak is no longer visible when  $\zeta = 0$  but it could be large if  $\zeta$  were increased.

The effect of the sine shape of the bellows can be seen in Fig. b7 where  $d1=0.02$ ; the second support peak is larger than in Fig. b1. This effect is further accentuated in Fig. b8 when  $d2=0.02$  where there is also a peak at  $\omega l = 2\pi$  at  $4 \times 450 = 1800$  psi which here is masked by the second support peak. In addition to  $\zeta$  and  $d1$ , the presence of  $d2$  contributes to the rise of the curve even at operating pressure.

Table 1: Pressure (psi) values at peaks

$k_{t1}$	3e7 lb in/radian	1e4 lb in/radian
$\omega l = \pi$ peak	450	450
$\omega l = 2\pi$ peak	1800	1800
$k1, k_{t1a}$ peak	610	650, 1830
$k_{t1b}$ peak	1875	425

We determine next conditions for support stiffnesses such that support peaks remain always above the  $\omega l = \pi$  peak for any pressure. A conservative value for  $k_{t1}$  is given by the limit of  $k_{t1a}$  when  $k1$  is infinite and  $\omega = 0$ . This value is  $3D^2K/4$  for any value of  $k1$ , even infinity. The root  $k_{t1b}$  is zero at  $\omega l = \pi$  for all values of  $k1$ . Figure b3 can be used to verify that no peak will occur below  $\omega l = \pi$  if these guidelines are followed. Figure b4 indicates that the  $3D^2K/4$  value for  $k_{t1}$  is three times higher than needed in that figure to avoid low peaks. The torsional stiffness for an SSC dipole with two support posts is estimated in the next section at  $1.5e7$  lb in/radian which is much higher than the  $4.6e5$  lb in/radian obtained from the proposed limit  $k_{t1} = 3D^2K/4$ .

## VI. Numerical Results: Bellows interactions in Magnet Systems

### Magnet equivalent Stiffness

In order to relate results from the magnet bellows system to the spring-supported model it is desirable to have an approximate value for the equivalent lateral spring constant and torsional stiffness of the magnet ends.

The magnet is modeled as an axially compressed beam with five supports to which a force or moment is applied at one end. This is a classical statistically indeterminate problem solved by applying the equations derived in Section III for the magnet-bellows assembly to one magnet only.

One of the major differences (of concern to us in this problem) between dipoles and quadrupoles lies in the location and number of supports which is adjusted by setting the relevant support stiffnesses to zero in the general model with five supports. Entries in Table 2 show stiffnesses for SSC dipoles mounted on five supports inside the cryostat which itself is mounted on two

supports to the ground. (The cryostats are interconnected by bellows.) The actual stiffness of the magnet-cryostat assembly is between the two extreme cases of five supports and two supports. Tests can be made to measure the stiffness of the magnet-cryostat assembly. The lateral stiffness  $k$ , and torsional stiffness  $k_t$  are practically linear functions of the axial force equivalent to the pressure, but their increase is so small that they can be considered constant.

Table 2: Magnet stiffness

Magnet	k lb/in	$k_t$ lb in/radian
SSC dipole 5 support	6300	$3.0 e7$
SSC dipole 2 support	530	$1.5e7$

### Magnet bellows assembly

The first example of a magnet bellows assembly is for a dipole-dipole-dipole combination with SSC dimensions. The bellows inner diameter is 14.3 in, its length is 9.3 in, and the axial stiffness which will produce a first peak at 450 psi is  $K=2760$  lb/in, the precompression  $\lambda=1$  in, the safety factor over the operating pressure of 300 psi is thus 1.5. In Fig. d1 the maximum local elongation of the two bellows is plotted versus pressure, the initial offset of the first bellows is  $\zeta_6=0.03$  in, it has an initially bent shape with  $d_{6s}=0.02$  and  $d_{6e}=0.02$  in. The upper curve made of triangles corresponds to the first bellows, the lower curve made of crosses corresponds to the second bellows. Maximum elongations are denoted in the legend  $dl_a$  and  $dl_b$  for the first and second bellows respectively, all values are truncated at 5 in for better display of details.

### Peaks

There is a small peak in the curve for the first bellows at 450 psi which requires a fine mesh to be detected. It reveals the indeterminacy at  $\omega l = \pi$  discussed in the spring-supported model. The rate of rise to this  $\omega l = \pi$  peak is controlled by  $\zeta$ ,  $d_{6s}$  and  $d_{6e}$ . There is a rising trend in the curve as it proceeds toward the  $\omega l = 2\pi$  peak at 1800 psi.

The curve corresponding to the first bellows (which has the mounting offset) shows a large rise to the first support peak at 600 psi. The second bellows has a smaller peak at the same location but does not seem to rise below that. This indicates very little, if any, interaction between bellows. Going back to Fig. b2, a peak at about 600 psi for large  $k_t$  would occur at  $k1=6000$  lb/in. This number agrees with the 6300 lb/in computed above in the section on magnet equivalent stiffness.

### Mounting and shape of bellows

Figure d2 shows the ideal case where there are no

mounting offsets and where the bellows are almost straight. Comparison with Fig. d1 shows that as with the spring-supported model,  $\zeta_{6,7,13,14}$ ,  $\eta_{6,7,13,14}$  and  $d_{6,13}$ ,  $d_{6,13}$  increase the rate of rise to the support peak. The effect of an initial angle  $\eta$  is similar to the effect of  $\zeta$ , for instance replacing  $\zeta_6=0.03$  by  $\eta_6=0.004$  would leave Fig. d1 unchanged. If both bellows were mounted in the same manner and had the same initial shapes, then the lower curve of Fig. d1 would coincide with the upper one. In the spring-supported model (Fig. b6) there was no visible support peak when  $\zeta=0$ , but there is one here because the assembly was assumed to have an initial average parabolic shape due to the magnets' sagitta.

#### Bellows interaction

Figure d3 corresponds to the case where lateral forces ( $f(7)=-f(6)=12500$  p/p<sub>op</sub> if  $p \leq p_{op}$  and  $f(7)=-f(6)=12500$  lbs if  $p \geq p_{op}$ ) are applied to the first bellows according to Fig. 9 in order to simulate failure in a dipole-dipole-dipole assembly. The upper bellows curve has exceeded the 5 in cutoff limit while the lower bellows curve remains flat denoting no interaction between adjacent bellows at operating pressure. A more pronounced interaction effect is visible in Fig. d4 for the dipole-quadrupole-dipole assembly where the second bellows shows a maximum elongation of 0.5 in above the initial precompression of 1 in. Complete failure of one bellows does not cause adjacent bellows to fail.

#### Deflected shape of assembly and bellows

Figure d5 shows the deflected shape of the assembly corresponding to Fig. d1 at operating pressure. In order to better see the effect of the internal pressure on the system, only the departure  $y$  of the assembly from the initial shape has been plotted. The total final shape is the superposition of the initial parabolic shape, the sine and cosine bellows shapes if they apply, and  $y$ . The 0.03 in offset marks the end of the first dipole and the beginning of the first bellows. The offset can also be seen in the bellows deflected shape in Fig. d6.

The two types of instabilities which can occur, the Euler-type of buckling and that due to the support system have been identified. The support peak (or peaks) should always be above the  $\omega\ell = \pi$  peak, this is controlled mostly by ensuring a large value for the torsional stiffness of the bellows supports. Interaction between bellows affects only support peaks which are kept well above the 450 psi ( $\omega\ell = \pi$ ).

#### REFERENCES

- [1] P. Seide, "The effect of Pressure on the Bending Characteristics of an Actuator System, Journal of Applied Mechanics," Sept. 1960, pp.429-437.
- [2] J.A. Haringx, "Instability of Thin Walled Cylinders Subjected to Internal Pressure," Philips Research Reports, vol. 7, 1952, pp.112-118.
- [3] J.A. Haringx, "Instability of Bellows Subjected to Internal Pressure," Philips Research Reports, vol. 7, 1952, pp.189-196.

### DISCLAIMER

This report was prepared as an account of work sponsored by an agency of the United States Government. Neither the United States Government nor any agency thereof, nor any of their employees, makes any warranty, express or implied, or assumes any legal liability or responsibility for the accuracy, completeness, or usefulness of any information, apparatus, product, or process disclosed, or represents that its use would not infringe privately owned rights. Reference herein to any specific commercial product, process, or service by trade name, trademark, manufacturer, or otherwise does not necessarily constitute or imply its endorsement, recommendation, or favoring by the United States Government or any agency thereof. The views and opinions of authors expressed herein do not necessarily state or reflect those of the United States Government or any agency thereof.

$$\text{determinant} = f_a \left( \frac{1}{k_2} + \frac{1}{k_1} \right) \cos(\alpha) + \frac{f_a (f_a - f_v) \sin(\alpha)}{k_1 k_2} + f_v \left( \frac{1}{k_2} + \frac{1}{k_1} \right) \sin(\alpha) - f_v \cos(\alpha)$$

$$= f_a \left( \frac{1}{k_2} + \frac{1}{k_1} \right) \cos(\alpha) + \frac{1}{k_2} \left( \frac{1}{k_1} \right) (\sin(\alpha) - \cos(\alpha)) - \frac{f_a \sin(\alpha)}{k_1 k_2} + f_v \left( \frac{1}{k_2} + \frac{1}{k_1} \right) (1 - \cos(\alpha))$$

$$= 0 \quad (1 - \cos(\alpha) + 2 \cos(\alpha) - 1)$$

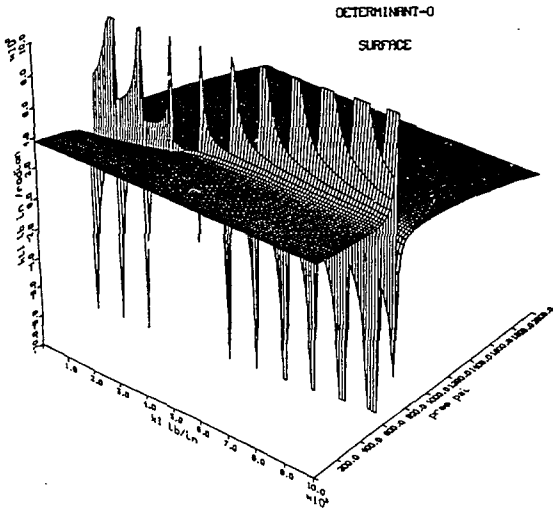


FIGURE E1

Spring Supported model:  $k_1$  vs Pres

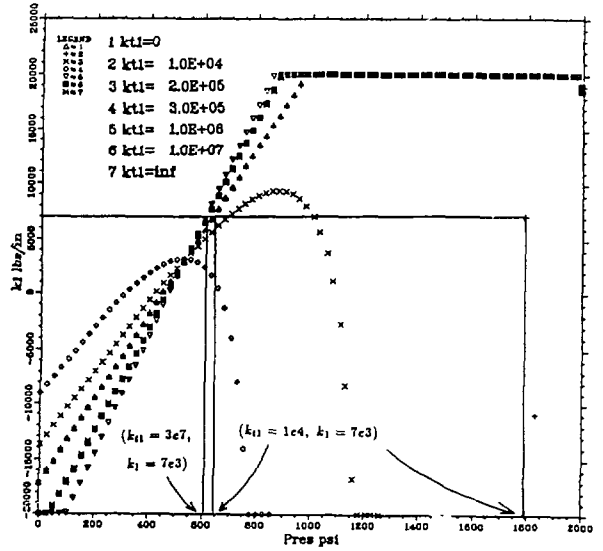


FIGURE B2

Spring-supported Bellows model: max elong vs pres

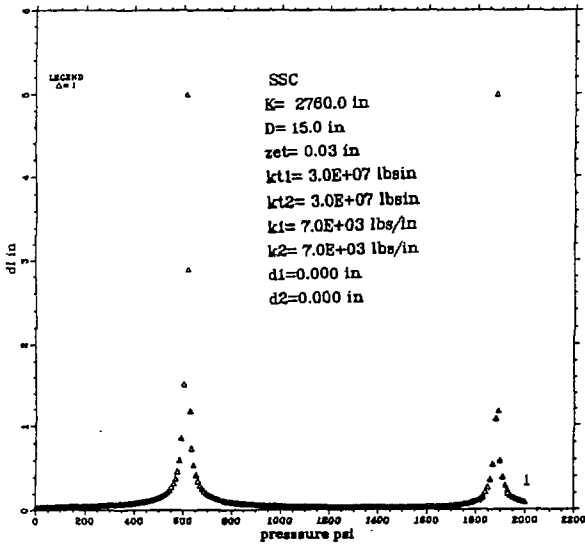


FIGURE B1

Spring Supported model:  $kt_{1a}$  vs Pres

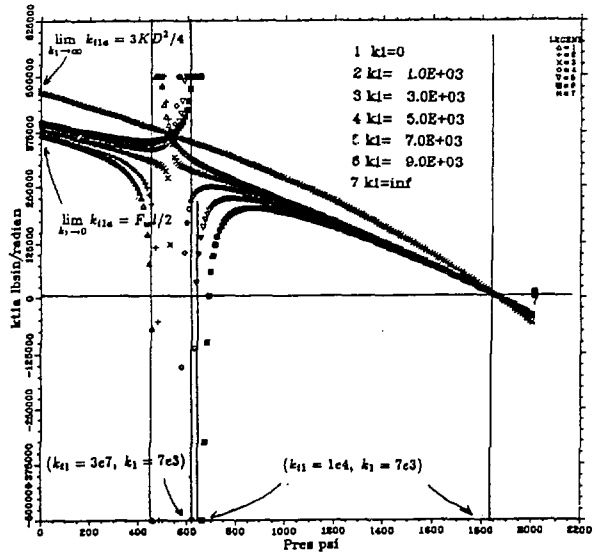


FIGURE B3

Spring Supported model:  $kt/b$  vs Pres

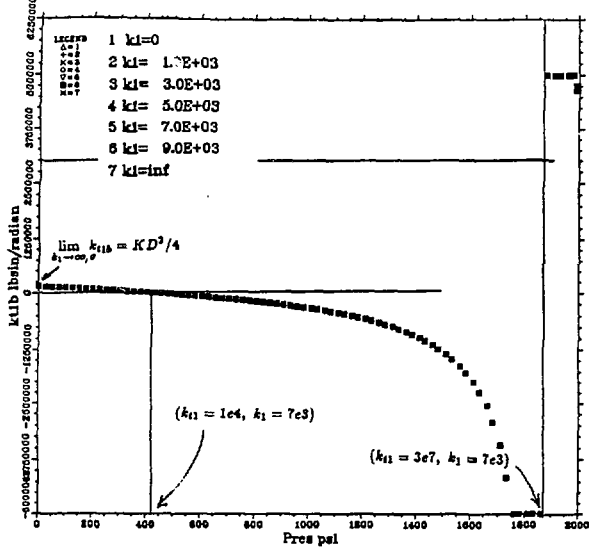


FIGURE B4

Spring-supported Bellows model: max elong vs pres

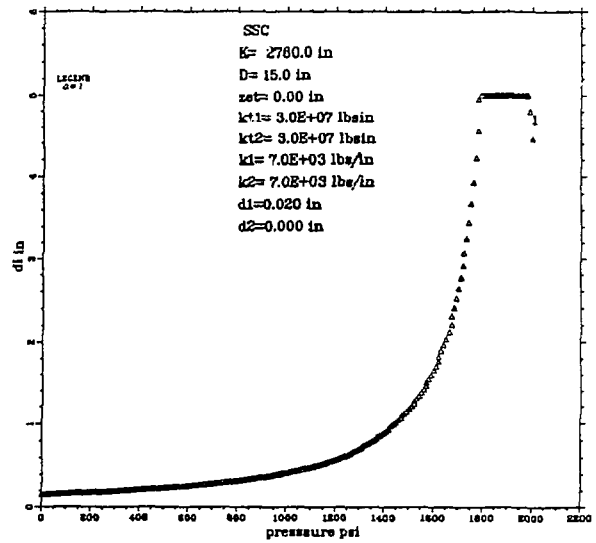


FIGURE B6

Spring-supported Bellows model: max elong vs pres

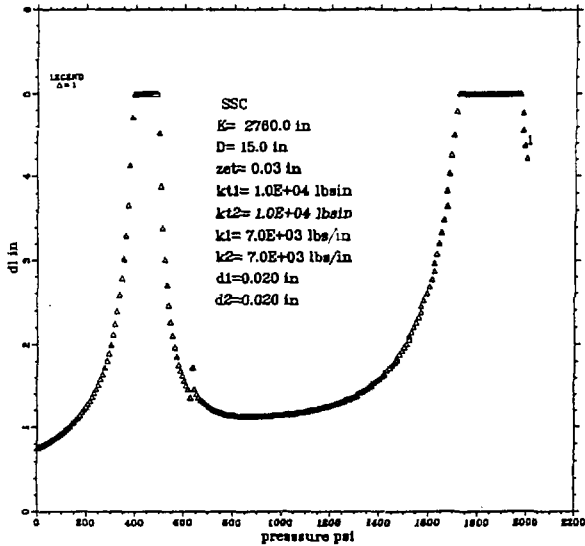


FIGURE B5

Spring-supported Bellows model: max elong vs pres

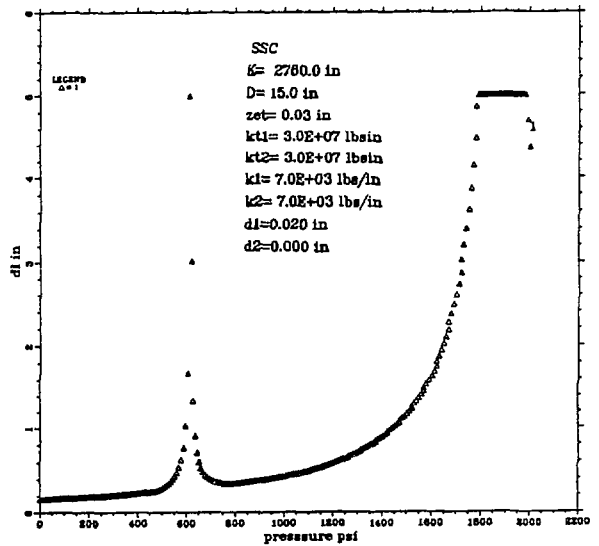


FIGURE B7

Spring-supported Bellows model: max elong vs pres

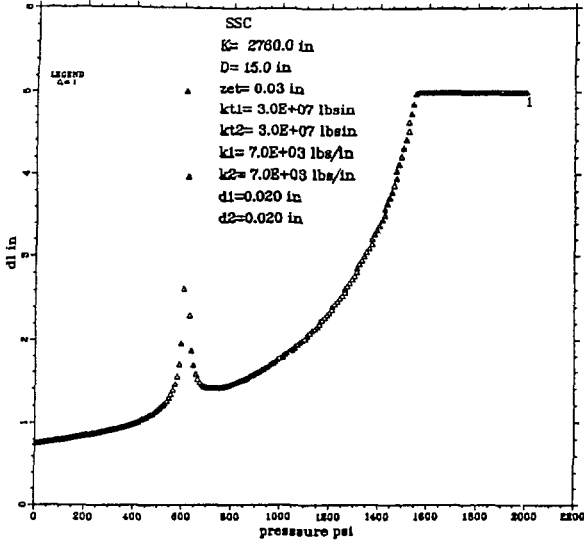


FIGURE B8

MAX BELLOWS LOCAL ELONGATION

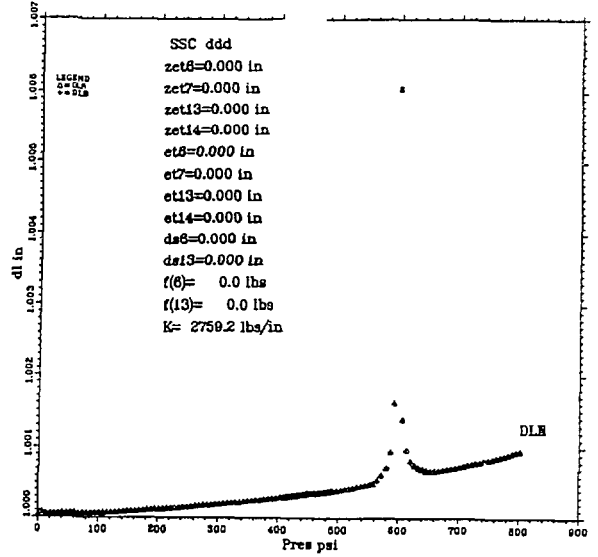


FIGURE D2

MAX BELLOWS LOCAL ELONGATION

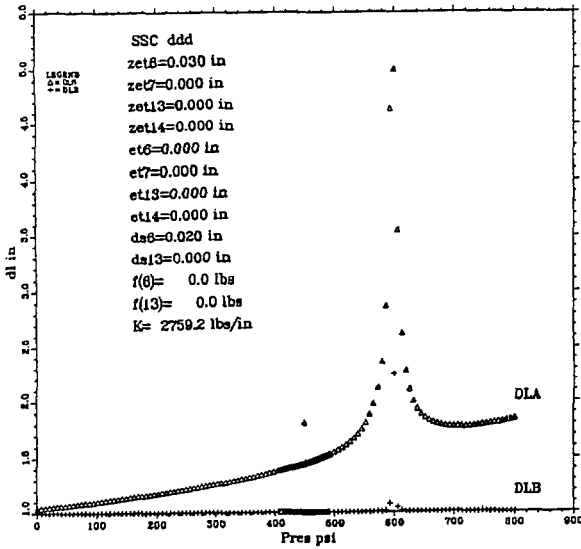


FIGURE D1

MAX BELLOWS LOCAL ELONGATION

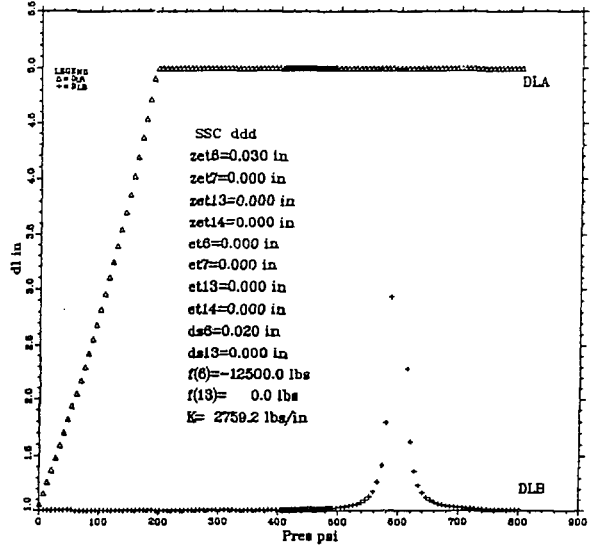
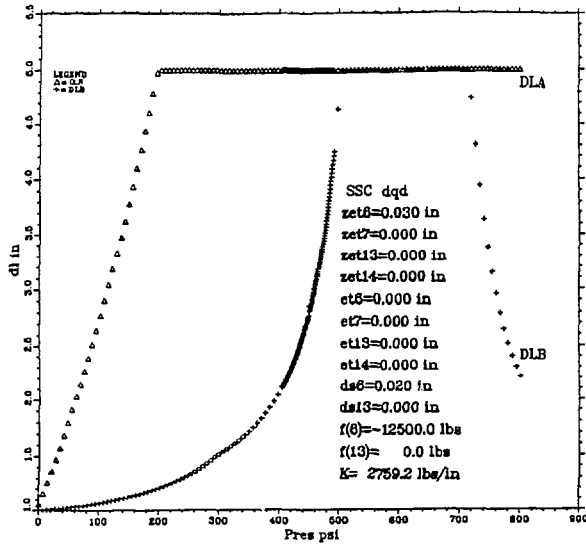


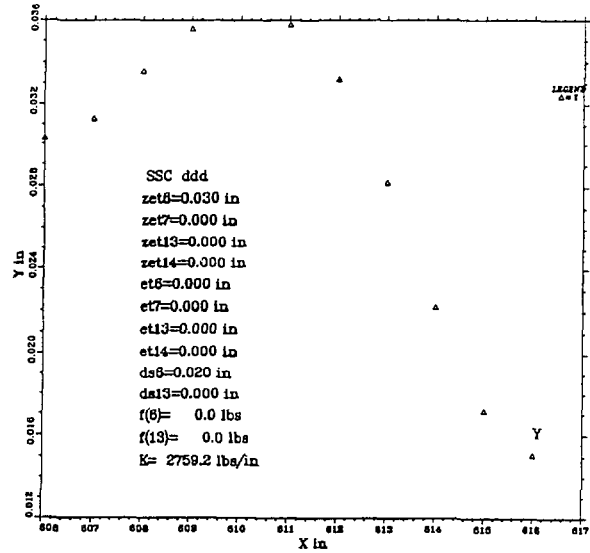
FIGURE D3

MAX BELLOWS LOCAL ELONGATION



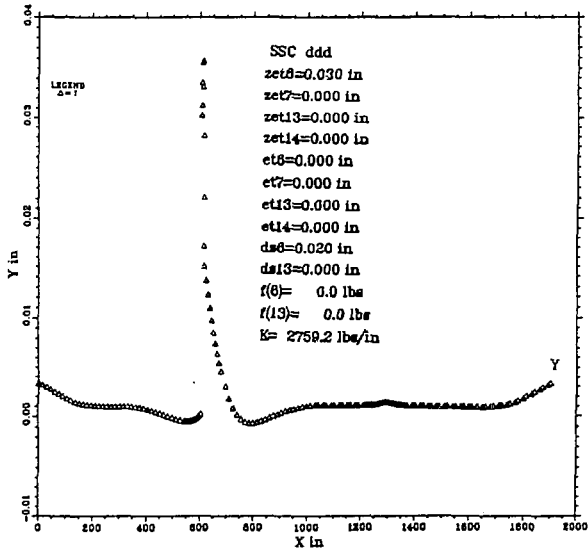
##DUAT7<ROSSUM.BUC>POR001.DAT;10 FIGURE D4

FIRST BELLOWS DEFLECTION AT 300 psi



##DUAT7<ROSSUM.BUC>POR001.DAT;00 FIGURE D6

ASSEMBLY DEFLECTIONS AT 303.5 psi



##DUAT7<ROSSUM.BUC>POR001.DAT;00 FIGURE D5